JACS
JOURNAL OF THE AMERICAN CHEMICAL SOCIETY
pubs.acs.org/JACS
Article

Overlap-Driven Splitting of Triplet Pairs in Singlet Fission

Elliot J. Taffet, David Beljonne, and Gregory D. Scholes*

Cite This: https://dx.doi.org/10.1021/jacs.0c09276
Read Online
ACCESS | Metrics & More | Article Recommendations | Supporting Information

ABSTRACT: We analyze correlated-triplet-pair (TT) singlet-fission intermediates toward two-triplet separation (T...T) using spin-state-averaged density matrix renormalization group electronic-structure calculations. Specifically, we compare the triplet−triplet exchange (J) for tetracene dimers, bipentacene, a subunit of the benzodithiophene−thiophene dioxide polymer, and a carotenoid (neurosporene). Exchange-split energy gaps of J and $3J$ separate a singlet from a triplet and a singlet from a quintet, respectively. We draw two new insights: (a) the canonical tetracene singlet-fission unit cell supports precisely three low-lying TT intermediates with order-of-magnitude differences in J, and (b) the separable TT intermediate in carotenoids emanates from a pair of excitations to the second triplet state. Therefore, unlike with tetracenes, carotenoid fission requires above-gap excitations. In all cases, the distinguishability of the molecular triplets—that is, the extent of orbital overlap—determines the splitting within the spin manifold of TT states. Consequently, J represents a spectroscopic observable that distnguishes the resemblance between TT intermediates and the T...T product.

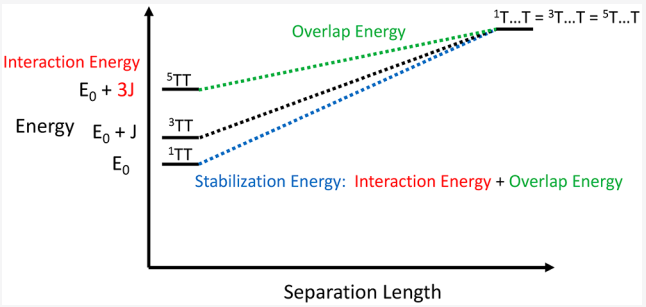

INTRODUCTION

Singlet fission (SF) exploits entanglement to make two from one—splitting a single-photon-absorbing state into two triplets.[1−6] This splitting has been phenomenologically recognized since the 1960s when the delayed fluorescence of anthracene and then crystalline tetracene was rationalized as the byproduct of annihilating two triplets.[7−10] Today, it is regarded as a potential breakthrough in the application of third-generation solar-cell technologies because of the capacity to transcend the Shockley−Queisser efficiency limit through charge-carrier duplication.[11,12] Yet what marks SF two-triplet production is unclear.[1,13,14] The central question that this work is to address is how to quantify singlet-fission capacity—that is, the propensity to produce uncorrelated triplet excitations—of a nascent triplet pair (^{1}TT)[15] formed from a singlet excitation. Specifically, the energy splitting within the lowest-lying spin manifold of pair excitation states is calculated. When the splittings are small compared to perturbations that couple the states, the correlated triplet pair state is energetically predisposed toward decoherence into uncorrelated triplet excitations.

SF requires harvesting the spectrally distinguishable ^{1}TT intermediate,[16−19] serving as the spin-conserving bridge between the spin-singlet and spin-triplet manifolds,[13,20,21] as different molecular triplets. In the 1970s, ^{1}TT was identified as a dark excited state with symmetry identical to that of the ground state[22,23] —a doubly excited singlet state that may be accessible by two-photon excitation.[23−27] The first step of SF involves population transfer between the photoexcited and optically dark ^{1}TT excited states, featuring formally nonzero coupling in the face of a reduction in symmetry[28] or charge-resonance-mediated configuration interaction.[29−34] This necessary, but not sufficient, condition for SF precedes decoherence of ^{1}TT—itself a Fermionic singlet eigenstate comprised of indistinguishable triplet excitations—into two separate decoupled triplet subsystem eigenstates.[6] The extensively reported two-intermediate mechanism of singlet fission[35] is

$$S^* \rightleftharpoons [TT \rightleftharpoons T...T] \rightleftharpoons T_1 + T_1$$

where S* represents the initially photoexcited state, TT represents the nascent intermediate, T...T represents the spatial product of SF,[1,13,36] and $T_1 + T_1$ represents the two-triplet product of SF.

For SF to produce two distinct, uncorrelated, triplet excitations, TT should be spatially decoupled (T...T)[35,37,38] so as to enable mixing between degenerate spin states.[13] This spin-mixed wave function is a simple product state of spatial wave functions localized on each molecule without correlations between the molecular triplet spins. One can view the pair as spin-disentangled by scrambling electronic population among its spin-singlet, -triplet, and -quintet realizations.[6,39] The production of uncoupled triplet excitations by spin decoher-

Received: August 28, 2020

Table 1. Summary of the Lowest-Energy Pair Excitation States

state	approximate composition	pair state spin eigenfunction[a]	excitation energy[b]
$\|X_1\rangle$	^{1}TT	$\frac{1}{\sqrt{3}}\left[\theta_1 + \theta_6 - \frac{1}{2}\left(\theta_2 + \theta_3 + \theta_4 + \theta_5\right)\right]$	$2E_0 - 2J_0 + J$
$\|Z_{3,M=0}\rangle$	^{3}TT	$\frac{1}{\sqrt{2}}\left(\theta_1 - \theta_6\right)$	$2E_0 - 2J_0$
$\|Q_{M=0}\rangle$	^{5}TT	$\frac{1}{\sqrt{6}}\left(\theta_1 + \theta_2 + \theta_3 + \theta_4 + \theta_5 + \theta_6\right)$	$2E_0 - 2J_0 - 2J$

[a]Basis functions θ_j are detailed in ref 13. [b]J_0 is half the singlet−triplet splitting of the monomer. The triplet−triplet exchange depends on interchromophore orbital overlap (refs 1 and 14): $J = (J_{ll} + J_{hh} + J_{lh} + J_{hl})/2$, where "l" denotes the lowest unoccupied molecular orbital and "h" the highest occupied molecular orbital.

ence helps to decouple ^{1}TT from the singlet manifold and suppresses decay to the identically symmetric ground state.[16−18,30]

In this report, we compare the differences in the orbital overlap-dependent contribution to the triplet−triplet exchange splitting[40] (*vide infra*), which gives quantitative insight into the energetic barrier to TT spin-state decoherence. We refer to triplet−triplet exchange splitting as J. The strategy utilized in this work is to use single-point computation of the noninteracting ^{5}TT state[41] as a proxy for the T...T spatial product[42] that represents a totally degenerate TT spin manifold.[43] That is, computing ^{5}TT clues us in to how close ^{1}TT is to T...T. This approach provides key physical insight into the extent to which singlet-configurational interaction contributes to ^{1}TT.[44] Configuration interaction within the singlet manifold, caused by electronic overlap, distinguishes ^{1}TT from ^{5}TT, and, in turn, the nonoverlapping T...T product, energetically and compositionally (for a recent conceptual review of this mixing, see Young and Wasielewski).[45] Therefore, the gap between the two-triplet product and ^{1}TT intermediate can be gleaned from the energetic nondegeneracy within the TT spin manifold. This experimental observable[16,17] is the triplet−triplet exchange splitting (J).

COMPUTATIONAL DETAILS

Density matrix renormalization group (DMRG) electronic-structure calculations using Block[46−48] (Version 1.1.1) interfaced with PySCF[49] with bond-dimension 1000 and DFT ground-state molecular geometry optimizations using Gaussian 16[50−71] were performed with the cc-pVDZ basis. DFT ground-state geometric optimizations were performed with the B3LYP functional. TIPS−tetracene crystal-structure geometries were used in the electronic-structure calculations.

Reported calculations on the carotenoid neurosporene involved DMRG(18,18)−SCF[72] orbital optimization averaging the lowest five singlets, lowest two triplets, and lowest quintet, followed by state-specific NEVPT2 with the compressed matrix-product-state perturber function.[73] The choice of states was based on the minimal averaging required to include the excited singlets of interest: $1B_u$, $2A_g$, $2B_u$, and $3A_g$. Moreover, the choice of method was meant to balance dynamic correlation for the bright and static correlation for the dark states, respectively. Yet, in this calculation, only the $2A_g$, $2B_u$, and $3A_g$ ^{1}TT states were computed as adjacent roots at the zeroth-order DMRG level. For reference, the bright-state excitation energy taken from smaller-active-space three-singlet-state-averaged DMRG(4,4)−NEVPT2, where only the $2A_g$ and $1B_u$ states were computed as adjacent roots at zeroth order, was included. Otherwise, calculations of triplet excitation energies and singlet−quintet TT energy splitting involved spin-state DMRG(4,4)−SCF orbital optimization averaging the lowest two singlets, lowest three triplets, and lowest quintet.

This methodology, predicated on averaging 2^1A_g (^{1}TT), ^3B_u (T_1), ^3A_g (T_2), ^{3}TT, and ^{5}TT together, was intended to calculate the TT manifold self-consistently. For avoidance of configuration contamination of ^{1}TT within calculations on the weakly overlapping tetracene dimers 4 and 5, the number of singlet states averaged at the DMRG(4,4)−SCF level of theory was increased to 4 and 3, respectively. Moreover, for improvement of the computational efficiency, tetracene dimer 4 was structurally truncated by replacing each triisopropylsilyl group with a hydrogen. Analysis of the zeroth-order DMRG wave functions was performed through inspection of the one- and two-particle reduced density and transition density matrices. Convergence in DMRG−SCF was achieved with a change in energy below 10^{-7} hartrees and in orbital gradient below 10^{-4} hartrees. Total energies of all converged states were computed to within 10^{-11} hartrees. Initial-guess orbitals for the (4,4) active space were generated from a Hartree−Fock calculation, while for larger active spaces, they were obtained from smaller-active-space DMRG−SCF converged orbitals.[74,75]

RESULTS AND DISCUSSION

Intermolecular Singlet Fission within the Weak-Coupling Regime. We focus on the crystalline unit cell of triisopropylsilyl (TIPS)−tetracene for which the triplet−triplet exchange interaction J underlying the pair has been experimentally resolved.[18]

Correlated pair states can be thought of as the combined electronic state of two molecules supporting four unpaired electrons. In prior work,[13] the branching diagram method was used to calculate spin eigenfunctions of the states, showing the manifold comprises one triplet pair that is an overall singlet $|X_1\rangle$, one singlet pair that is an overall singlet $|X_2\rangle$, one set of triplet-pair states with an overall quintet spin $|Q_j\rangle$, $j = -2, -1, 0, +1, +2$, and three sets of singlet−triplet pairs that are each an overall triplet $|Z_{n,j}\rangle$, $n = 1, 2, 3$ and $j = -1, 0, +1$. Recently, Tao and Tan[14] have constructed all triplet-pair excited-state wave functions from a four-unpaired-spin basis, but with two-triplet correlations included explicitly, to yield a ladder of TT-state energies split by the triplet−triplet exchange interaction (J). This interaction produces a multiexciton binding energy,[43] which is the energetic barrier from the interacting ^{1}TT to the noninteracting ^{5}TT state. Lowering this barrier may expedite the process of TT decoupling required to complete SF.[42]

https://dx.doi.org/10.1021/jacs.0c09276
J. Am. Chem. Soc. XXXX, XXX, XXX−XXX

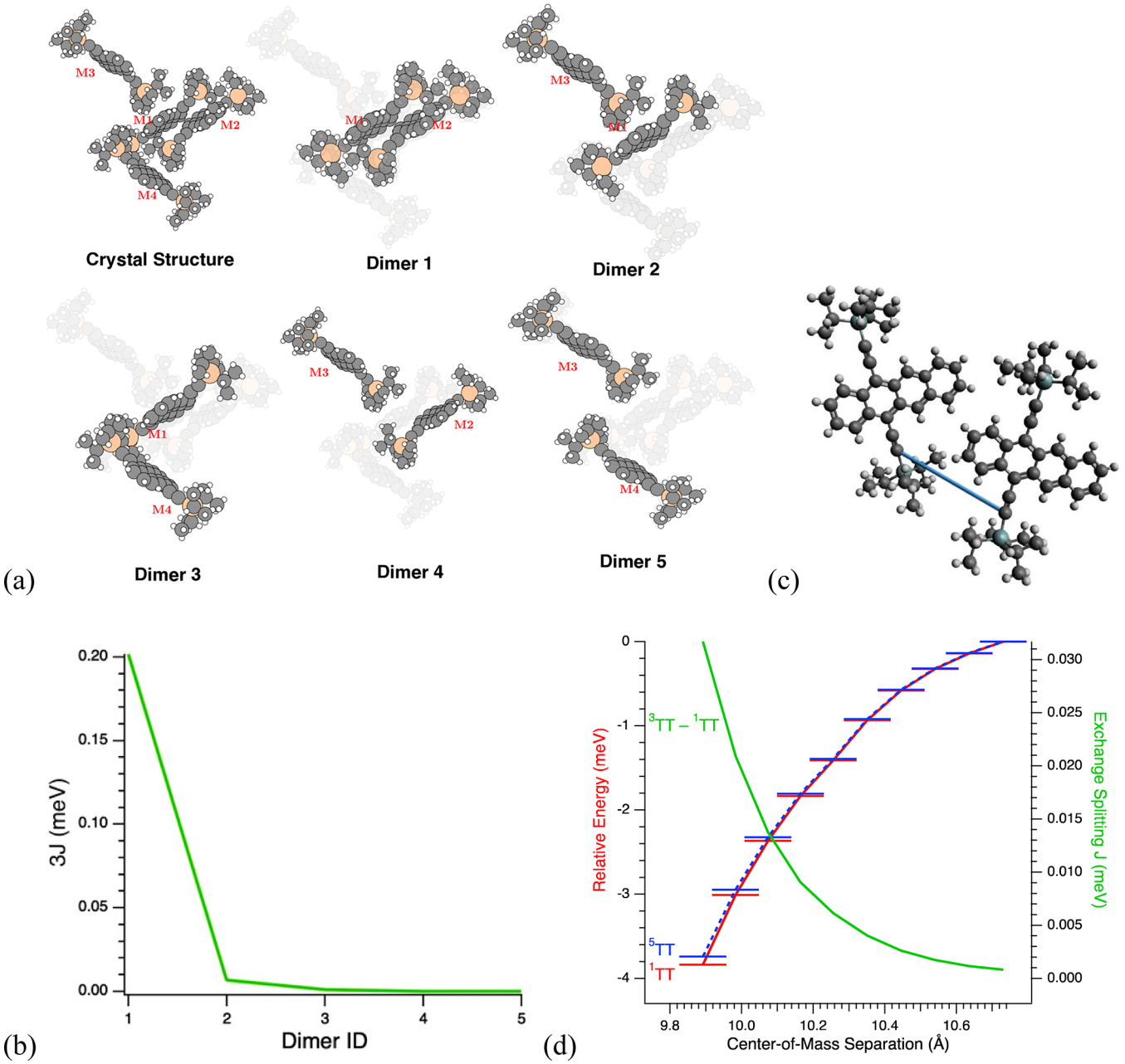

Figure 1. Differentiating TT states across different orientations of TIPS−tetracene dimers. (a) The five dimer-pair combinations within the TIPS−tetracene unit cell considered in this work. "M" indexes the four distinguishable monomers in the cell. (b) The energetic splitting between ^{5}TT and ^{1}TT ($3J$) for each dimer-pair combination (on a meV scale). (c) The displacement axis of dimer 1 used to generate the geometries analyzed in (d) because it leaves the intermonomer orientation unchanged with incremental center-of-mass separation. (d) Change in the energetics of the TT spin ladder caused by center-of-mass displacement.

In the present study, we compute the nonrelativistic transition energies for all lowest-lying (quasi-degenerate) TT spin states as correlated many-body wave functions,[76] arbitrarily for spin projection M = 0.[40] A summary of predictions[1,13,14] for these states is given in Table 1.

Our calculations of ^{5}TT−^{1}TT splitting ($3J$) corroborate the experimental result[18] of a closely coupled dimeric ^{1}TT state that is distinguishable within the unit cell by an order-of-magnitude larger triplet−triplet exchange interaction relative to those of the other dimers (Figure 1a,b).

We find a total of three different regimes of J across dimers 1, 2, and 3 in the 5-dimer combinatorial space we explore within the TIPS−tetracene unit cell (Figure 1b). Moreover, we discern precise energetic equivalency between ^{1}TT and ^{5}TT within dimers 4 and 5, intimating that the nonoverlapping T...T product can be realized from these dimer-pair combinations. To simulate the generation of this product from dimer 1, we displace the two monomers incrementally along the "slip" axis defined by the artificial bond between the alkynyl carbons highlighted in Figure 1c. At 10.7 Å separation between the monomeric centers of mass, J is reduced to a μeV—obfuscating the TT spin ladder in the face of intratriplet dipolar coupling (the D and E spectroscopic parameters)[77] that will commensurately split the spin states within ^{3}TT and within ^{5}TT. Thus, this large-separation-length limit approximates the T...T-product condition of degenerate spin-states, as

https://dx.doi.org/10.1021/jacs.0c09276
J. Am. Chem. Soc. XXXX, XXX, XXX−XXX

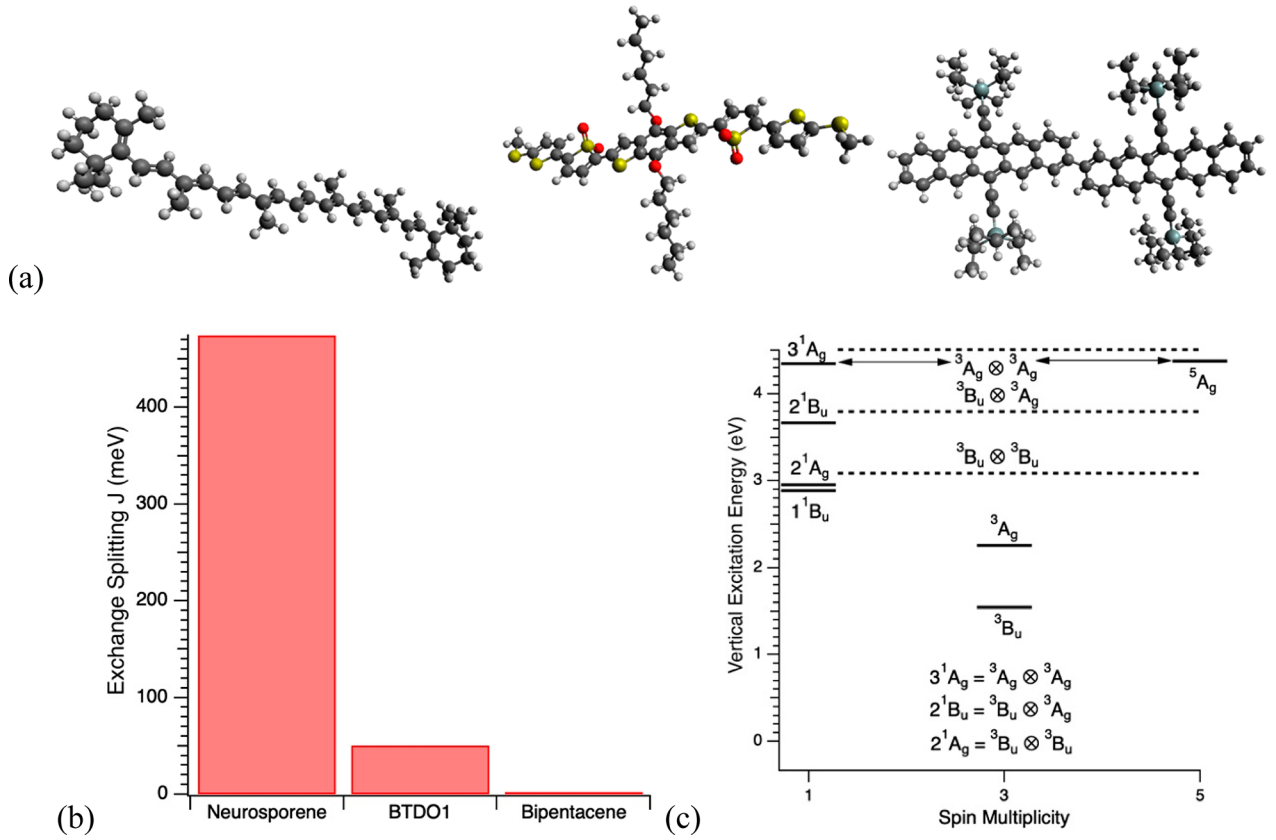

Figure 2. Comparative magnitudes of triplet−triplet exchange and excitation energies of TT states. (a) Molecular structures of (left to right) neurosporene, BTDO1, and bipentacene used for the calculations. (b) J, computed as one-third of the energetic difference between ^{5}TT and 2^1A_g in the optimized ground-state geometries. (c) The manifold of low-lying singlet, triplet, and quintet states (spin multiplicities 1, 3 and 5, respectively) in neurosporene. The group-theoretical relationships between the ^{1}TT states $\{2^1A_g, 2^1B_u, \text{and } 3^1A_g\}$ and their corresponding two-triplet excitations $\{^3B_u \text{ and } ^3A_g\}$ are enumerated. The excitation energies of the fictitious two-triplet states are plotted as dashed lines.

evidenced by the energetic convergence of ^{1}TT and ^{5}TT (Figure 1d).

The physical picture emanating from Figure 1d is one of an energetically ordered manifold of ^{1}TT, ^{3}TT, and ^{5}TT states that monotonically converge to the T...T excitation energy with increased spatial separation. Triplet−triplet exchange serves as the physical parameter that energetically positions the spin states in the order $^1\text{TT} < {}^3\text{TT} < {}^5\text{TT}$ (the negative-exchange condition),[14] yielding the energetic relations $^1\text{TT} = {}^3\text{TT} - J = {}^5\text{TT} - 3J$ used spectroscopically.[18]

Note the meV scale of the triplet−triplet exchange J relative to the eV scale of singlet−triplet exchange (J_0) in SF systems.[13] In the adiabatic picture—where intermonomer overlap is inherent to the calculation of dimer-pair electronic structure—this theoretical exchange is revealed by calculating the spin-adapted states. We find that the sign of exchange is negative, which we interpret from the double-charge-transfer nature of the TT excitation (Supporting Information). For in the face of intermonomer overlap, the singlet charge-transfer (CT) configurations are stabilized through hybridization with locally excited (LE) character (drawing from the language of hybrid LE−CT states[78])—pushing the ^{1}TT adiabatic eigenstate down in energy toward $^3T_1$ (the so-called exciton binding energy[79]). Absolving the ^{1}TT state of all singlet mixing[19] renders it electronically, as well as spectrally, equivalent to a pair of triplet excitations.[1] Note that we have outlined here a framework for couplings within the 5-state spin-coupled model outlined in Tao.[80]

Intramolecular Singlet Fission within the Strong-Coupling Regime. Intramolecular SF is defined by strong coupling between covalently connected molecular units supporting the bimolecular TT state. We explore the effect of distinguishability between these units on J through comparative calculations on linearly coupled acenes (bipentacene),[81] a subunit of the canonical benzodithiophene−thiophene dioxide polymer ($BTDO_1$),[30] and a carotenoid (neurosporene).[74] These structures are displayed in Figure 2a; the geometries (in Cartesian coordinates) for these structures in their optimized ground states are provided in the Supporting Information. Note that our interest in determining, quantitatively, the energetic gaps *between* the ^{1}TT states of neurosporene necessitates dynamic- and static-correlation corrections, leading us to perform a spin-state-averaged DMRG−SCF/NEVPT2 calculation[73] with an 18-orbital, 18-electron active space. Yet for BTDO1 and bipentacene, where our interest is in the relative splitting *within* the lowest-lying TT manifold, we apply the same DMRG−SCF method as before with a 4-orbital, 4-electron active space. We find that J increases with relative indistinguishability of the molecular units (from bipentacene to neurosporene) as a result of stronger overlap-driven configuration interaction along the purely one-dimensional conjugated path in neurosporene (Figure 2b).

In all three cases, J is larger than that found in the dimers of the model intermolecular SF system (TIPS−tetracene), but the spike in J found in neurosporene is due to a fundamental

https://dx.doi.org/10.1021/jacs.0c09276
J. Am. Chem. Soc. XXXX, XXX, XXX−XXX

change in the electronic stucture. Valentine et al.[82] recently noted that the configurational mixing underlying the lowest-lying ^{1}TT state renders the SF pathway obsolete. Instead, the TT manifestation in carotenoids should be thought of as a family of {2^1A_g, 2^1B_u, and 3^1A_g} triplet-pair excitations, with the latter constituting the SF intermediate state in carotenoids and the former constituting that in conjugated polymers (such as $BTDO_1$) and acenes. Here, the labels correspond to the irreducible representations of the canonical C_{2h} point-group symmetry that characterizes these planarized, highly conjugated SF chromophores with a 1^1A_g ground state.[1] Nonetheless, as is the case with all SF systems, the neurosporene 2^1A_g state lies energetically closest to the 1^1B_u bright state.[74]

The implication of TT configurational mixing in carotenoids (Figure 2b) is that, as observed recently through pump-push-probe spectroscopy, optical pumping above the main absorption band of carotenoids is necessary to activate the SF pathway.[83] We can make sense of this experimental result by observing that, in agreement with the result of Valentine et al.,[82] the 3^1A_g state, while energetically furthest from the bright 1^1B_u state, is energetically closest to ^{5}TT (^5A_g)—separated by ^{a} ^{5}TT−^{1}TT splitting ($3J$) on the same meV-scale computed for acenes. Such a result suggests that the 3^1A_g state, which uniquely is defined as the superposition of two T_2 (^3A_g) excitations (Figure 2c), is a TT state that effectively resembles a double excitation of two triplets localized on either half of the polyenic chain.[24] That is, we observe a correspondence between T_2 of the full system and T_1 of the half system computed in Valentine et al.[82] In contrast, 2^1A_g is made up of T_1 excitations delocalized over the full system, connecting its energetic divergence from the noninteracting ^{5}TT state to excitonic effects between the two coupled chain halves.[13] Therefore, the carotenoid 3^1A_g state likely serves as the TT intermediate in intramolecular SF.

In summary, TT spin-state rungs on the energetic ladder leading to the T...T SF product of degenerate states proceed in the following order from bottom to top: ^{1}TT, ^{3}TT, and ^{5}TT. The ^{5}TT intermediate falls below the T...T product because of underlying nonlocality of the putatively molecular triplets—that is, intermolecular orbital overlap. This "overlap energy" (which makes the triplets indistinguishable) can be understood as lowering the energy of each individual triplet comprising the TT state through one-electron transfer integrals between the molecular frontier orbitals.[6] In physical terms, this coupling spreads each triplet wave function across the bimolecular pair, thereby decreasing the triplet transition energy—and concomitantly lowering the ^{5}TT = T_1 + T_2 transition energy. Note that only the energetic correction due to overlap (the terms of order "S^2" in Scholes,[13] where "S" is the overlap integral) differentiates the ^{5}TT energy from the T...T energy, which is equivalent to twice the monomer triplet energy for a homodimer. As previously mentioned, the ^{5}TT state is noninteracting[41] —there are no other configurations to be coupled to TT in the quintet manifold. Consequently, the internal splitting *within* a TT spin manifold, unique to the overlap inherent to a given intermonomer spatial separation and orientation, manifests because of the unique *singlet* configuration interaction ("interaction energy") enabled by quasidegenerate locally excited states and generally higher-lying charge-resonance states in the singlet manifold. While higher-lying charge-resonance configurations may also electronically couple to ^{3}TT, the unique second-order mediated configuration interaction between singlets, in which one-electron couplings to charge-resonance configurations support the mixing between local excitations and ^{1}TT, causes ^{1}TT to split off from ^{5}TT and lie below ^{3}TT. Therefore, we may disentangle the overlap-driven stabilization of the entire TT spin manifold from the overlap-dependent configuration interaction that splits the manifold as follows: ^{1}TT = ^{3}TT − J = ^{5}TT − $3J$.

CONCLUSION

There are two essential physical parameters that split the manifolds of TT states in space and spin: overlap energy (stabilizing the entire TT spin manifold relative to T...T) and interaction energy (stabilizing the mixed ^{1}TT state relative to the noninteracting ^{5}TT state). The latter is responsible for the experimentally observable triplet−triplet exchange (J) derived from frontier-orbital delocalization across the two monomers supporting the bimolecular TT state. In the weak-coupling regime, this delocalization causes the 2^1A_g state of SF systems to fall below the ^5A_g state on the meV scale; in the strong-overlap regime, however, substantial excitonic effects render the ^5A_g state energetically inaccessible from the lower-lying 2^1A_g TT excitation.

ASSOCIATED CONTENT

Supporting Information

The Supporting Information is available free of charge at https://pubs.acs.org/doi/10.1021/jacs.0c09276.

Physical properties of the optimized DMRG TT wave functions; analysis of the Davydov splitting within the triplet and singlet manifolds; influence of outlying correlation in neurosporene calculations (PDF)

AUTHOR INFORMATION

Corresponding Author

Gregory D. Scholes − *Department of Chemistry, Princeton University, Princeton, New Jersey 08544, United States;* orcid.org/0000-0003-3336-7960; Email: gscholes@princeton.edu

Authors

Elliot J. Taffet − *Department of Chemistry and the PULSE Institute, Stanford University, Stanford, California 94305, United States; SLAC National Accelerator Laboratory, Menlo Park, California 94025, United States;* orcid.org/0000-0002-8321-5116

David Beljonne − *Department of Chemistry, University of Mons, 7000 Mons, Belgium;* orcid.org/0000-0002-2989-3557

Complete contact information is available at: https://pubs.acs.org/10.1021/jacs.0c09276

Notes

The authors declare no competing financial interest.

ACKNOWLEDGMENTS

E.J.T. acknowledges Prof. Todd J. Martinez for a postdoctoral fellowship and thanks Dr. Leah R. Weiss for discussions and helpful analysis concerning the experimental resolution of triplet−triplet exchange splittings in polycrystalline TIPS−tetracene.

https://dx.doi.org/10.1021/jacs.0c09276
J. Am. Chem. Soc. XXXX, XXX, XXX−XXX

REFERENCES

(1) Miyata, K.; Conrad-Burton, F. S.; Geyer, F. L.; Zhu, X.-Y. Triplet Pair States in Singlet Fission. *Chem. Rev.* **2019**, *119* (6), 4261−4292.

(2) Gish, M. K.; Pace, N. A.; Rumbles, G.; Johnson, J. C. Emerging Design Principles for Enhanced Solar Energy Utilization with Singlet Fission. *J. Phys. Chem. C* **2019**, *123* (7), 3923−3934.

(3) Krishnapriya, K. C.; Roy, P.; Puttaraju, B.; Salzner, U.; Musser, A. J.; Jain, M.; Dasgupta, J.; Patil, S. Spin Density Encodes Intramolecular Singlet Exciton Fission in Pentacene Dimers. *Nat. Commun.* **2019**, *10* (1), 33.

(4) Lee, T. S.; Lin, Y. L.; Kim, H.; Rand, B. P.; Scholes, G. D. Two Temperature Regimes of Triplet Transfer in the Dissociation of the Correlated Triplet Pair after Singlet Fission. *Can. J. Chem.* **2019**, *97* (6), 465−473.

(5) Shen, C.; Yan, S.; Chen, X.; Niu, L.; Zhang, Y. Magnetic Field Effect on Singlet Exciton Fission: A Sensitive Probe of Molecular Level Morphology in Organic Films. *Org. Electron.* **2019**, *67*, 194−199.

(6) Smith, M. B.; Michl, J. Recent Advances in Singlet Fission. *Annu. Rev. Phys. Chem.* **2013**, *64*, 361−386.

(7) Singh, S.; Jones, W. J.; Siebrand, W.; Stoicheff, B. P.; Schneider, W. G. Laser Generation of Excitons and Fluorescence in Anthracene Crystals. *J. Chem. Phys.* **1965**, *42*, 330−342.

(8) Swenberg, C. E.; Stacy, W. T. Bimolecular Radiationless Transitions in Crystalline Tetracene. *Chem. Phys. Lett.* **1968**, *2*, 327−328.

(9) Merrifield, R. E.; Avakian, P.; Groff, R. P. Fission of Singlet Excitons into Pairs of Triplet Excitons in Tetracene Crystals. *Chem. Phys. Lett.* **1969**, *3*, 386−388.

(10) Geacintov, N.; Pope, M.; Vogel, F. Effect of Magnetic Field on the Fluorescence of Tetracene Crystals: Exciton Fission. *Phys. Rev. Lett.* **1969**, *22*, 593−596.

(11) Shockley, W.; Queisser, H. J. Detailed Balance Limit of Efficiency of P-n Junction Solar Cells. *J. Appl. Phys.* **1961**, *32*, 510−519.

(12) Hanna, M. C.; Nozik, A. J. Solar Conversion Efficiency of Photovoltaic and Photoelectrolysis Cells with Carrier Multiplication Absorbers. *J. Appl. Phys.* **2006**, *100*, 074510.

(13) Scholes, G. D. Correlated Pair States Formed by Singlet Fission and Exciton-Exciton Annihilation. *J. Phys. Chem. A* **2015**, *119*, 12699−12705.

(14) Tao, G.; Tan, Y. Modular Tensor Diagram Approach for the Construction of Spin Eigenfunctions: The Case Study of Exciton Pair States. *J. Phys. Chem. A* **2020**, *124* (26), 5435−5443.

(15) Kim, H. M.; Zimmerman, P. Coupled Double Triplet State in Singlet Fission. *Phys. Chem. Chem. Phys.* **2018**, *20* (48), 30083−30094.

(16) Weiss, L. R.; Bayliss, S. L.; Kraffert, F.; Thorley, K. J.; Anthony, J. E.; Bittl, R.; Friend, R. H.; Rao, A.; Greenham, N. C.; Behrends, J. Strongly Exchange-Coupled Triplet Pairs in an Organic Semiconductor. *Nat. Phys.* **2017**, *13* (2), 176.

(17) Bayliss, S. L.; Weiss, L. R.; Rao, A.; Friend, R. H.; Chepelianskii, A. D.; Greenham, N. C. Spin Signatures of Exchange-Coupled Triplet Pairs Formed by Singlet Fission. *Phys. Rev. B: Condens. Matter Mater. Phys.* **2016**, *94* (4), 045204.

(18) Bayliss, S. L.; Weiss, L. R.; Mitioglu, A.; Galkowski, K.; Yang, Z.; Yunusova, K.; Surrente, A.; Thorley, K. J.; Behrends, J.; Bittl, R.; Anthony, J. E.; Rao, A.; Friend, R. H.; Plochocka, P.; Christianen, P. C. M.; Greenham, N. C.; Chepelianskii, A. D. Site-Selective Measurement of Coupled Spin Pairs in an Organic Semiconductor. *Proc. Natl. Acad. Sci. U. S. A.* **2018**, *115* (20), 5077−5082.

(19) Yong, C. K.; Musser, A. J.; Bayliss, S. L.; Lukman, S.; Tamura, H.; Bubnova, O.; Hallani, R. K.; Meneau, A.; Resel, R.; Maruyama, M.; Hotta, S.; Herz, L. M.; Beljonne, D.; Anthony, J. E.; Clark, J.; Sirringhaus, H. The Entangled Triplet Pair State in Acene and Heteroacene Materials. *Nat. Commun.* **2017**, *8*, 15953.

(20) Smith, M. B.; Michl, J. Singlet Fission. *Chem. Rev.* **2010**, *110*, 6891−6936.

(21) Piland, G. B.; Burdett, J. J.; Dillon, R. J.; Bardeen, C. J. Singlet Fission: From Coherences to Kinetics. *J. Phys. Chem. Lett.* **2014**, *5* (13), 2312−2319.

(22) Schulten, K.; Karplus, M. On the Origin of a Low-Lying Forbidden Transition in Polyenes and Related Molecules. *Chem. Phys. Lett.* **1972**, *14*, 305−309.

(23) Hudson, B. S.; Kohler, B. E. A Low-Lying Weak Transition in the Polyene α,ω-Diphenyloctatetraene. *Chem. Phys. Lett.* **1972**, *14*, 299−304.

(24) Tavan, P.; Schulten, K. Electronic Excitations in Finite and Infinite Polyenes. *Phys. Rev. B: Condens. Matter Mater. Phys.* **1987**, *36*, 4337−4358.

(25) Schulten, K.; Ohmine, I.; Karplus, M. Correlation Effects in the Spectra of Polyenes. *J. Chem. Phys.* **1976**, *64* (11), 4422−4441.

(26) Tavan, P.; Schulten, K. The 2 1Ag-1 1Bu Energy Gap in the Polyenes: An Extended Configuration Interaction Study. *J. Chem. Phys.* **1979**, *70* (12), 5407−5413.

(27) Tavan, P.; Schulten, K. The Low-lying Electronic Excitations in Long Polyenes: A PPP-MRD-CI Study. *J. Chem. Phys.* **1986**, *85*, 6602−6609.

(28) Matsika, S.; Feng, X.; Luzanov, A. V.; Krylov, A. I. What We Can Learn from the Norms of One-Particle Density Matrices, and What We Can't: Some Results for Interstate Properties in Model Singlet Fission Systems. *J. Phys. Chem. A* **2014**, *118* (51), 11943−11955.

(29) Beljonne, D.; Yamagata, H.; Brédas, J. L.; Spano, F. C.; Olivier, Y. Charge-Transfer Excitations Steer the Davydov Splitting and Mediate Singlet Exciton Fission in Pentacene. *Phys. Rev. Lett.* **2013**, *110* (22), 226402.

(30) Busby, E.; Xia, J.; Wu, Q.; Low, J. Z.; Song, R.; Miller, J. R.; Zhu, X. Y.; Campos, L. M.; Sfeir, M. Y. A Design Strategy for Intramolecular Singlet Fission Mediated by Charge-Transfer States in Donor-Acceptor Organic Materials. *Nat. Mater.* **2015**, *14*, 426−433.

(31) Berkelbach, T. C.; Hybertsen, M. S.; Reichman, D. R. Microscopic Theory of Singlet Exciton Fission. I. General Formulation. *J. Chem. Phys.* **2013**, *138* (11), 114102.

(32) Berkelbach, T. C.; Hybertsen, M. S.; Reichman, D. R. Microscopic Theory of Singlet Exciton Fission. II. Application to Pentacene Dimers and the Role of Superexchange. *J. Chem. Phys.* **2013**, *138* (11), 114103.

(33) Chan, W.-L.; Berkelbach, T. C.; Provorse, M. R.; Monahan, N. R.; Tritsch, J. R.; Hybertsen, M. S.; Reichman, D. R.; Gao, J.; Zhu, X.-Y. The Quantum Coherent Mechanism for Singlet Fission: Experiment and Theory. *Acc. Chem. Res.* **2013**, *46* (6), 1321−1329.

(34) Chan, W.-L.; Ligges, M.; Jailaubekov, A.; Kaake, L.; Miaja-Avila, L.; Zhu, X.-Y. Observing the Multiexciton State in Singlet Fission and Ensuing Ultrafast Multielectron Transfer. *Science* **2011**, *334* (6062), 1541−1545.

(35) Lee, T. S.; Lin, Y. L.; Kim, H.; Pensack, R. D.; Rand, B. P.; Scholes, G. D. Triplet Energy Transfer Governs the Dissociation of the Correlated Triplet Pair in Exothermic Singlet Fission. *J. Phys. Chem. Lett.* **2018**, *9* (14), 4087−4095.

(36) Srimath Kandada, A. R.; Petrozza, A.; Lanzani, G. Ultrafast Dissociation of Triplets in Pentacene Induced by an Electric Field. *Phys. Rev. B: Condens. Matter Mater. Phys.* **2014**, *90* (7), 075310.

(37) Pensack, R. D.; Ostroumov, E. E.; Tilley, A. J.; Mazza, S.; Grieco, C.; Thorley, K. J.; Asbury, J. B.; Seferos, D. S.; Anthony, J. E.; Scholes, G. D. Observation of Two Triplet-Pair Intermediates in Singlet Exciton Fission. *J. Phys. Chem. Lett.* **2016**, *7*, 2370−2375.

(38) Pensack, R. D.; Tilley, A. J.; Grieco, C.; Purdum, G. E.; Ostroumov, E. E.; Granger, D. B.; Oblinsky, D. G.; Dean, J. C.; Doucette, G. S.; Asbury, J. B.; Loo, Y.-L.; Seferos, D. S.; Anthony, J. E.; Scholes, G. D. Striking the Right Balance of Intermolecular Coupling for High-Efficiency Singlet Fission. *Chemical Science* **2018**, *9* (29), 6240−6259.

(39) Suna, A. Kinematics of Exciton-Exciton Annihilation in Molecular Crystals. *Phys. Rev. B* **1970**, *1* (4), 1716−1739.

(40) Mayhall, N. J. From Model Hamiltonians to Ab Initio Hamiltonians and Back Again: Using Single Excitation Quantum

https://dx.doi.org/10.1021/jacs.0c09276
J. Am. Chem. Soc. XXXX, XXX, XXX−XXX

Chemistry Methods To Find Multiexciton States in Singlet Fission Materials. *J. Chem. Theory Comput.* **2016**, *12* (9), 4263−4273.
(41) Casanova, D. Theoretical Modeling of Singlet Fission. *Chem. Rev.* **2018**, *118*, 7164−7207.
(42) Kolomeisky, A. B.; Feng, X.; Krylov, A. I. A Simple Kinetic Model for Singlet Fission: A Role of Electronic and Entropic Contributions to Macroscopic Rates. *J. Phys. Chem. C* **2014**, *118* (10), 5188−5195.
(43) Feng, X.; Luzanov, A. V.; Krylov, A. I. Fission of Entangled Spins: An Electronic Structure Perspective. *J. Phys. Chem. Lett.* **2013**, *4* (22), 3845−3852.
(44) Zimmerman, P. M.; Zhang, Z.; Musgrave, C. B. Singlet Fission in Pentacene through Multi-Exciton Quantum States. *Nat. Chem.* **2010**, *2* (8), 648.
(45) Young, R. M.; Wasielewski, M. R. Mixed Electronic States in Molecular Dimers: Connecting Singlet Fission, Excimer Formation, and Symmetry-Breaking Charge Transfer. *Acc. Chem. Res.* **2020**, *53* (9), 1957−1968.
(46) Chan, G. K.-L.; Head-Gordon, M. Highly Correlated Calculations with a Polynomial Cost Algorithm: A Study of the Density Matrix Renormalization Group. *J. Chem. Phys.* **2002**, *116*, 4462−4476.
(47) Chan, G. K.-L. An Algorithm for Large Scale Density Matrix Renormalization Group Calculations. *J. Chem. Phys.* **2004**, *120*, 3172−3178.
(48) Sharma, S.; Chan, G. K.-L. Spin-Adapted Density Matrix Renormalization Group Algorithms for Quantum Chemistry. *J. Chem. Phys.* **2012**, *136*, 124121.
(49) Sun, Q.; Berkelbach, T. C.; Blunt, N. S.; Booth, G. H.; Guo, S.; Li, Z.; Liu, J.; McClain, J. D.; Sayfutyarova, E. R.; Sharma, S.; Wouters, S.; Chan, G. K.-L. PySCF: The Python-Based Simulations of Chemistry Framework. *Wiley Interdiscip. Rev.: Comput. Mol. Sci.* **2018**, *8* (1), No. e1340.
(50) Frisch, M. J.; Trucks, G. W.; Schlegel, H. B.; Scuseria, G. E.; Robb, M. A.; Cheeseman, J. R.; Scalmani, G.; Barone, V.; Petersson, G. A.; Nakatsuji, H.; Li, X.; Caricato, M.; Marenich, A. V.; Bloino, J.; Janesko, B. G.; Gomperts, R.; Mennucci, B.; Hratchian, H. P.; Ortiz, J. V.; Izmaylov, A. F.; Sonnenberg, J. L.; Williams; Ding, F.; Lipparini, F.; Egidi, F.; Goings, J.; Peng, B.; Petrone, A.; Henderson, T.; Ranasinghe, D.; Zakrzewski, V. G.; Gao, J.; Rega, N.; Zheng, G.; Liang, W.; Hada, M.; Ehara, M.; Toyota, K.; Fukuda, R.; Hasegawa, J.; Ishida, M.; Nakajima, T.; Honda, Y.; Kitao, O.; Nakai, H.; Vreven, T.; Throssell, K.; Montgomery, J. A., Jr.; Peralta, J. E.; Ogliaro, F.; Bearpark, M. J.; Heyd, J. J.; Brothers, E. N.; Kudin, K. N.; Staroverov, V. N.; Keith, T. A.; Kobayashi, R.; Normand, J.; Raghavachari, K.; Rendell, A. P.; Burant, J. C.; Iyengar, S. S.; Tomasi, J.; Cossi, M.; Millam, J. M.; Klene, M.; Adamo, C.; Cammi, R.; Ochterski, J. W.; Martin, R. L.; Morokuma, K.; Farkas, O.; Foresman, J. B.; Fox, D. J. *Gaussian 16*; Gaussian Inc.: Wallingford, CT, 2016.
(51) Hohenberg, P.; Kohn, W. Inhomogeneous Electron Gas. *Phys. Rev.* **1964**, *136*, B864−B871.
(52) Kohn, W.; Sham, L. J. Self-Consistent Equations Including Exchange and Correlation Effects. *Phys. Rev.* **1965**, *140*, A1133−A1138.
(53) Parr, R. G.; Yang, W. *Density-Functional Theory of Atoms and Molecules*; International Series of Monographs on Chemistry 16; Oxford University Press: New York, 1989; Vol. *16*.
(54) In *The Challenge of d and f Electrons: Theory and Computation*; Reinhold, J. D. R., Salahub, M. ACS Symposium Series 394; American Chemical Society: Washington, DC, 1989; *Cryst. Res. Technol.* 1990, *25* (6) 624−624. DOI: 10.1002/crat.2170250603.
(55) Dixon, D. A.; Andzelm, J.; Fitzgerald, G.; Wimmer, E.; Jasien, P.; Labanowski, J.; Andzelm, J. W. *Density Functional Methods in Chemistry*; Springer: Berlin, 1991; pp 33−56.
(56) Andzelm, J.; Wimmer, E. Density Functional Gaussian-type-orbital Approach to Molecular Geometries, Vibrations, and Reaction Energies. *J. Chem. Phys.* **1992**, *96*, 1280−1303.
(57) Becke, A. D. Density-functional Thermochemistry. I. The Effect of the Exchange-only Gradient Correction. *J. Chem. Phys.* **1992**, *96*, 2155−2160.
(58) Perdew, J. P.; Wang, Y. Accurate and Simple Analytic Representation of the Electron-Gas Correlation Energy. *Phys. Rev. B: Condens. Matter Mater. Phys.* **1992**, *45*, 13244−13249.
(59) Scuseria, G. E. Comparison of Coupled-cluster Results with a Hybrid of Hartree-Fock and Density Functional Theory. *J. Chem. Phys.* **1992**, *97*, 7528−7530.
(60) Becke, A. D. Density-functional Thermochemistry. II. The Effect of the Perdew-Wang Generalized-gradient Correlation Correction. *J. Chem. Phys.* **1992**, *97*, 9173−9177.
(61) Gill, P. M.; Johnson, B. G.; Pople, J. A.; Frisch, M. J. The Performance of the Becke—Lee—Yang—Parr (B—LYP) Density Functional Theory with Various Basis Sets. *Chem. Phys. Lett.* **1992**, *197*, 499−505.
(62) Perdew, J. P.; Chevary, J. A.; Vosko, S. H.; Jackson, K. A.; Pederson, M. R.; Singh, D. J.; Fiolhais, C. Atoms, Molecules, Solids, and Surfaces: Applications of the Generalized Gradient Approximation for Exchange and Correlation. *Phys. Rev. B: Condens. Matter Mater. Phys.* **1992**, *46*, 6671−6687.
(63) Perdew, J. P.; Chevary, J. A.; Vosko, S. H.; Jackson, K. A.; Pederson, M. R.; Singh, D. J.; Fiolhais, C. Erratum: Atoms, Molecules, Solids, and Surfaces: Applications of the Generalized Gradient Approximation for Exchange and Correlation. *Phys. Rev. B: Condens. Matter Mater. Phys.* **1993**, *48*, 4978−4978.
(64) Sosa, C.; Lee, C. Density Functional Description of Transition Structures Using Nonlocal Corrections. Silylene Insertion Reactions into the Hydrogen Molecule. *J. Chem. Phys.* **1993**, *98* (10), 8004−8011.
(65) Stephens, P. J.; Devlin, F. J.; Chabalowski, C. F.; Frisch, M. J. Ab Initio Calculation of Vibrational Absorption and Circular Dichroism Spectra Using Density Functional Force Fields. *J. Phys. Chem.* **1994**, *98*, 11623−11627.
(66) Stephens, P. J.; Devlin, F. J.; Ashvar, C. S.; Chabalowski, C. F.; Frisch, M. J. Theoretical Calculation of Vibrational Circular Dichroism Spectra. *Faraday Discuss.* **1994**, *99*, 103−119.
(67) Ricca, A.; Bauschlicher, C. W. Successive H2O Binding Energies for Fe(H2O)N+. *J. Phys. Chem.* **1995**, *99*, 9003−9007.
(68) Pople, J. A.; Gill, P. M. W.; Johnson, B. G. Kohn—Sham Density-Functional Theory within a Finite Basis Set. *Chem. Phys. Lett.* **1992**, *199*, 557−560.
(69) Johnson, B. G.; Frisch, M. J. Analytic Second Derivatives of the Gradient-Corrected Density Functional Energy. Effect of Quadrature Weight Derivatives. *Chem. Phys. Lett.* **1993**, *216*, 133−140.
(70) Johnson, B. G.; Fisch, M. J. An Implementation of Analytic Second Derivatives of the Gradient-corrected Density Functional Energy. *J. Chem. Phys.* **1994**, *100*, 7429−7442.
(71) Stratmann, R. E.; Burant, J. C.; Scuseria, G. E.; Frisch, M. J. Improving Harmonic Vibrational Frequencies Calculations in Density Functional Theory. *J. Chem. Phys.* **1997**, *106*, 10175−10183.
(72) Ghosh, D.; Hachmann, J.; Yanai, T.; Chan, G. K.-L. Orbital Optimization in the Density Matrix Renormalization Group, with Applications to Polyenes and *β*-Carotene. *J. Chem. Phys.* **2008**, *128*, 144117.
(73) Guo, S.; Watson, M. A.; Hu, W.; Sun, Q.; Chan, G. K.-L. N-Electron Valence State Perturbation Theory Based on a Density Matrix Renormalization Group Reference Function, with Applications to the Chromium Dimer and a Trimer Model of Poly(p-Phenylenevinylene). *J. Chem. Theory Comput.* **2016**, *12*, 1583−1591.
(74) Taffet, E. J.; Lee, B. G.; Toa, Z. S. D.; Pace, N.; Rumbles, G.; Southall, J.; Cogdell, R. J.; Scholes, G. D. Carotenoid Nuclear Reorganization and Interplay of Bright and Dark Excited States. *J. Phys. Chem. B* **2019**, *123* (41), 8628−8643.
(75) Taffet, E. J.; Fassioli, F.; Toa, Z. S. D.; Beljonne, D.; Scholes, G. D. Uncovering Dark Multichromophoric States in Peridinin-Chlorophyll-Protein. *J. R. Soc., Interface* **2020**, *17* (164), 20190736.

https://dx.doi.org/10.1021/jacs.0c09276
J. Am. Chem. Soc. XXXX, XXX, XXX−XXX

(76) Zimmerman, P. M.; Musgrave, C. B.; Head-Gordon, M. A Correlated Electron View of Singlet Fission. *Acc. Chem. Res.* **2013**, *46* (6), 1339−1347.
(77) Zahlan, A. B. *The Triplet State*; Google Books (accessed 2020-08-18).
(78) Gibson, J.; Monkman, A. P.; Penfold, T. J. The Importance of Vibronic Coupling for Efficient Reverse Intersystem Crossing in Thermally Activated Delayed Fluorescence Molecules. *ChemPhysChem* **2016**, *17* (19), 2956−2961.
(79) Trinh, M. T.; Zhong, Y.; Chen, Q.; Schiros, T.; Jockusch, S.; Sfeir, M. Y.; Steigerwald, M.; Nuckolls, C.; Zhu, X. Intra- to Intermolecular Singlet Fission. *J. Phys. Chem. C* **2015**, *119*, 1312−1319.
(80) Tao, G. Topology of Quantum Coherence in Singlet Fission: Mapping out Spin Micro-States in Quasi-Classical Nonadiabatic Simulations. *J. Chem. Phys.* **2020**, *152* (7), 074305.
(81) Sanders, S. N.; Kumarasamy, E.; Pun, A. B.; Trinh, M. T.; Choi, B.; Xia, J.; Taffet, E. J.; Low, J. Z.; Miller, J. R.; Roy, X.; Zhu, X. Y.; Steigerwald, M. L.; Sfeir, M. Y.; Campos, L. M. Quantitative Intramolecular Singlet Fission in Bipentacenes. *J. Am. Chem. Soc.* **2015**, *137*, 8965−8972.
(82) Valentine, D. J.; Manawadu, D.; Barford, W. Higher-Energy Triplet-Pair States in Polyenes and Their Role in Intramolecular Singlet Fission. *Phys. Rev. B: Condens. Matter Mater. Phys.* **2020**, *102* (12), 125107.
(83) Pandya, R.; Gu, Q.; Cheminal, A.; Chen, R. Y. S.; Booker, E. P.; Soucek, R.; Schott, M.; Legrand, L.; Mathevet, F.; Greenham, N.; Barisien, T.; Musser, A.; Chin, A. W.; Rao, A. Optical Projection and Spatial Separation of Spin Entangled Triplet-Pairs from the S_1 ($2^1A_g^-$) State of Pi-Conjugated Systems. *Chem* **2020**, *6* (10), 2826−2851.

https://dx.doi.org/10.1021/jacs.0c09276
J. Am. Chem. Soc. XXXX, XXX, XXX−XXX